



# **NUMERICAL MODELING OF REINFORCED EARTH WALLS: INFLUENCE OF SOIL CONSTITUTIVE MODELS ON STRUCTURAL BEHAVIOR AND DISPLACEMENT**

**Cherif Guergah<sup>1,2</sup>, Adam Hamrouni<sup>3</sup>, and Sarah Djouimaa<sup>4</sup>**

**<sup>1</sup> Department of Civil Engineering/ Mohamed-Cherif Messaadia University/ Souk Ahras/ Algeria, Email:guergah.cherif@yahoo.fr.**

**<sup>2</sup> Laboratory of Civil Engineering and Hydraulics/Guelma University/Algeria.**

**<sup>3</sup> Laboratory InfraRES/ Mohammed Cherif Messaadia University/ Souk-Ahras/ Algeria  
Email:hamrouni.adam@yahoo.fr.**

**<sup>4</sup> Laboratory InfraRES/ Mohammed Cherif Messaadia University/ Souk-Ahras/ Algeria  
Email:s.djouimaa@univ-soukahras.dz.**

**<https://doi.org/10.30572/2018/KJE/170114>**

## **ABSTRACT**

In geotechnical engineering, reinforced soil walls are preferred due to their economical advantage and versatility. Nonetheless, the determination of the structural response of reinforced soil walls under different loading states remains a challenge, especially concerning the selection of an adequate soil constitutive model. This paper describes the development of a two-dimensional computational model capable of examining the effect of soil constitutive models on the structural response of reinforced soil walls. This study utilized a precise simulation of the design process, combining the results with soil parameters obtained through experiments. Two soil constitutive models are considered: the Mohr-Coulomb (MC) model, which is a linear elastic-perfectly plastic model widely used in geotechnical engineering, and the Cap-Yield (CYsoil) soil constitutive model, which captures the soil nonlinearity and stress-dependent stiffness. Results reveal the significant effect of the soil constitutive models on the general response of the structure, including the soil displacement field. Specifically, the MC soil model, which simplifies the shear strength of the soil, overestimates the soil stiffness, predicting lower soil displacements. On the contrary, the CYsoil soil model, which captures the soil nonlinearity, stress-dependent stiffness, and plastic volumetric strains, provides predictions of larger soil displacements. The obtained results highlight the role of selecting a suitable soil



model in designing reinforced earth structures. This work has shown that including non-linear soil behavior improves simulation accuracy in numerical modeling for geotechnical problems.

**KEYWORDS**

Reinforced Earth Wall; Numerical Modeling; Constitutive Models; Mohr-Coulomb Model; Cap-Yield Model; Nonlinear Analysis.

## 1. INTRODUCTION

Reinforced earth walls can be applied as a remedy for geotechnical issues, owing to their ability to provide an economic and stable retention system design. Retention systems act because of interactions that occur between soil and reinforcement. However, simulation for such systems is done using appropriate approaches related to numerical methods as well as soil equations.

In conventional analysis, the strategies used in the design of the wall may incorporate simple assumptions, which may fail to properly represent the forces at play in the soil structure interaction. Currently, with the rise in the use of computational analysis, the analysis of the structure using numerical analysis tools has become essential in determining the mechanics of the walls, particularly in the area of Reinforced earth walls structures.

The numerical analysis of reinforced earth structures dated back to the 1970s, where main attention was concentrated on inextensible metallic reinforcements in walls. However, over the years, numerical techniques such as FEM or FDM have gained popularity to predict soil mechanics in reinforced walls in research works carried out by several authors, and they include (Clough & James in 1971, Chang & Forsyth in 1977, Corté in 1977). Though these techniques can give significant data, significant variations in past research have been indicated by differences in modeling and inputs.

Numerical analysis techniques like the Finite Element Method (FEM), Finite Difference Method (FDM), etc., are employed for soil mechanics analysis of reinforced wall structures (Liu et al., 2011; Zhang et al., 2021). But conventional analysis techniques, which are primarily analytical, have limitations in obtaining accurate deformation conditions (Liu, 2016; Yousif and Mustafa, 2021; Fathipour et al., 2023).

Technological improvements have made it possible to make detailed analyses to further understand wall behavior and essential design parameters. Research studies focused on the effect of geometry parameters and reinforcements on the stability of the structure although differences exist because of varying parameters (Bastick, 1987; Ho and Rowe, 1994).

The two-dimensional numerical study ensures a high level of accuracy and remains computationally efficient (Ho and Rowe, 1994; Skinner and Rowe, 2005; Hatami and Bathurst, 2006; Bergado and Teerawattanasuk, 2008; Bathurst and Naftchali, 2021; Vibhoosha, 2021; Zhang et al., 2022; Xie et al., 2023). Not with standing the limitations, it can accurately describe essential structural interactions. This makes numerical techniques an integral tool in optimizing the design of a reinforced soil structure (Helwany et al., 1999; Allen and Bathurst, 2015; Hu and Li, 2024).

Numerical studies on the use of synthetic reinforcements with respect to the effect on the

stability and deformation of slopes have been extensively conducted (Ling et al., 2010; Liu et al., 2011; Yu et al., 2015; Bathurst & Naftchali, 2021; Morsy & Zornberg, 2021; Hamrouni et al., 2022). In spite of extensive studies on soil displacement, there are not many studies on the effect of different soil models on the behavior of reinforced soil slopes.

Numerical modeling has, in all likelihood, augmented the successes in designing the behavior of reinforced earth walls, but choosing the right model for the constitutive properties of the soil is critical to obtain reasonable predictions. The phenomenological mode of standard models, as in Mohr-Coulomb (MC), seems to show some discrepancies in relation to actual findings in experiments. This is because soil dilatancy, in general, is introduced in the constitutive model after the soil failure point. This point was well explained in various researches (Maji et al., 2016; Hosseininia and Ashjaee, 2018; Mašín, 2019; Hayal et al., 2021; Pande and Pietruszczak, 2021). Because dilatancy in general is considered after the soil's failure point. Hence, the mentioned types of models predict neither the rigidity for varying states of stresses nor predict any cycles of loading and unloading in the soil. Therefore, to adequately predict the mentioned complexities, there has been a suggestion for the adoption of advanced elastoplastic models involving "hardening", which provide a better balance in accuracy and availability of parameters in terms of triaxial test results.

This paper presents the analysis of reinforced earth walls using a two-dimensional numerical model developed within FLAC 2D, a finite difference method code. The model was calibrated with parameters derived from experimental investigations by (Abdelouhab et al., 2011; Abdelouhab et al., 2012a). A reference wall, first modeled and stabilized with synthetic reinforcements (Abdelouhab et al., 2012b), is analyzed here with realistic construction sequences and material properties through pullout and triaxial tests (Yang et al., 2010; Pham and Dias, 2021; Lafifi et al., 2024). An investigation into the influence of soil constitutive models-the Mohr-Coulomb model and the Cap-Yield model on the deformation behavior of reinforced earth walls under serviceability limit state conditions-is conducted herein.

The principal aim of this research is to investigate the effect of the choice of the constitutive model used in the simulation of the mechanical behavior of reinforced earth structures, particularly earth retaining structures like reinforced earth walls. A calibrated numerical model capable of simulating the mechanical behavior of reinforced earth walls under different levels of loading is used to compare the effect of the MC and CYsoil models and the effect of progressive construction sequences on embankments.

The essential mechanisms for designing the structure are incorporated into this model via the simulation of the step-by-step procedure for building both the reinforced wall and the

embankment. The implementation procedure is incorporated into this model via the addition of 0.375 m thick layers as follows:

- Placement of the first panel, the first and second layers, and the first reinforcement in-between the layers.
- Positioning of the third and fourth layers, as well as the addition of the second layer of reinforcement.
- Second panel installation, positioning of the fifth and sixth layers, and third reinforcement installation.

## 2. CONSTITUTIVE MODELS AND GEOMECHANICAL PARAMETERS FOR MODELING

The reference scenario is simulated using realistic geomechanical values. The interface properties between the soil and the reinforcement are established using the calibration process, with the laboratory pullout test results (Abdelouhab et al. 2012b). The reference values are described below.

### 2.1. Soil Characteristics

Reinforced Embankment and General Embankment: These regions are made of Hostun RF sand. This is a well-documented fine-grained uniform sand that is largely employed in geotechnical research (Flavigny et al., 1990; Gay et al., 2001). It has high uniformity and low percentages of fine materials. It is appropriate for a reinforced soil structure. It has well-characterized geotechnical properties, which include size, and angles of friction and permeability. These properties have been investigated in triaxial and direct shear tests in past research.

Foundation Soil: For the foundation soil, a linear elastic model is considered to behave like a homogeneous and isotropic material. This results in easier analysis with more practical load distribution patterns.

Values of the mechanical properties, including the elastic modulus (E), Poisson's ratio ( $\nu$ ), and the unit weight ( $\gamma$ ), of the soil materials have been provided in Table 1.

**Table 1. Geomechanical Characteristics of the Foundation Soil (Abdelouhab et al., 2011)**

Parameter	Symbol	Value	Unit	Description
Young's modulus	E	50	MPa	Stiffness of soil in the elastic range
Poisson's ratio	$\nu$	0.3	-	Ratio of lateral to axial strain
Density	$\rho$	2000	(kg/m <sup>3</sup> )	Mass per unit volume of soil

### 2.2. Mohr-Coulomb Model (MC)

The Mohr-Coulomb (MC) model is cast in the classical framework of incremental plasticity. Despite the constant stiffness values associated with loading and unloading processes, it is able

to reproduce the main properties of frictional materials with a reduced set of parameters. That is why it is conventionally employed in geotechnical engineering.

In this model, soil behavior can be categorized into two aspects:

Elastic Phase: This is governed by Hooke's law, having a Young's modulus of ( $E$ ), and a Poisson's ratio of ( $\nu$ ).

Plastic phase: This is described by the Mohr-Coulomb yield criterion, which is dependent on the internal friction angle ( $\phi$ ) and the cohesion ( $c$ ).

To circumvent the risk of overestimation of soil dilatancy, a plastic potential function is added. The plastic potential function adopts a dilatancy angle ( $\psi$ ), which is different from the friction angle ( $\phi$ ) used in the plasticity function (Zienkiewicz et al., 1975; Abdulhasan et al., 2020). The Mohr-Coulomb model requires five key parameters to define elastic-perfectly plastic behavior:

- Elastic parameters:  $E$  (Young's modulus),  $\nu$  (Poisson's ratio)
- Plastic parameters:  $\phi$  (Internal friction angle),  $c$  (Cohesion),  $\psi$  (Dilatancy angle)

### 2.3. CYsoil Model

The model CYsoil is a strain-hardening constitutive model that combines a frictional Mohr-Coulomb shear envelope, taken with zero cohesion, and an elliptic volumetric cap in the ( $p', q$ ) plane. This provides a more sophisticated modeling of the soil behavior compared to the classical Mohr-Coulomb model.

One of the salient features of the CYsoil model is that it takes into account:

- Cap-hardening law: Captures the volumetric power-law behavior observed in isotropic compaction tests.
- Compaction/dilation law: Represents the irrecoverable volumetric strain occurring due to soil shearing.
- Friction hardening law: Models hyperbolic stress-strain behavior, improving the accuracy of soil response under loading.

In this model, stiffness is stress-dependent, meaning it varies with effective confinement. As a result, stiffness is higher during unloading and reloading phases compared to initial loading, making this approach more suitable for capturing realistic stress-dependent soil behavior.

If friction hardening behavior is adopted, the required input parameters include (ITASCA, 2011):

- Elastic tangent shear modulus  $G_{\text{ref}}^e$  at a reference effective pressure ( $p^{\text{ref}} = 100 \text{ KPa}$ ):

$$G_{\text{ref}}^e = E / (2(1 + \mu)) \quad (1)$$

- Elastic tangent bulk modulus  $K_{\text{ref}}^e$  at a reference effective pressure ( $p^{\text{ref}} = 100 \text{ KPa}$ ):

$$K_{\text{ref}}^e = E / (3(1 - 2\mu)) \quad (2)$$

- Failure ratio  $R_f$  which is a constant and smaller than 1
- Ultimate friction angle  $\varphi_f$
- Calibration factor  $\beta$

The behavior of both the reinforced backfill and the general backfill is modeled using two distinct approaches:

1. Linear elastic perfectly plastic model based on the Mohr-Coulomb (MC) failure criterion.
2. Nonlinear elasticity model with a Cap-Yield (CYsoil) failure criterion.

The parameters for these models were determined through calibration based on triaxial tests conducted in the laboratory on Hostun sand. These tests were performed under different confining pressures: 30 kPa, 60 kPa, and 90 kPa.

To calibrate the parameters of the MC and CYsoil models, numerical simulations of triaxial tests were carried out at various depths corresponding to the reference case. The results of this calibration are summarized in [Table 2](#).

[Fig. 1](#) presents the stress-strain curves obtained for different values of  $\sigma_3$ . For the numerical analyses in this study, the CYsoil model parameters corresponding to a confining pressure of 47.5 kPa; which represents a depth of 6 m at the base of the wall; were selected [Table 2](#).

**Table 2. Geomechanical Properties of Hostun Sand for Mohr-Coulomb and CYsoil models**

MC model	Value	CYsoil model	Value
E (Young's modulus) (MPa)	50	Reference elastic tangent shear modulus $G_{ref}^e$ (MPa)	19.25
$\nu$ (Poisson ratio)	0.3	Elastic tangent shear modulus $G^e$ (MPa) $G^e = G_f^e(\sigma_3/P^{ref})$	9.15
$\varphi$ (friction angle) (degrees)	36	Elastic tangent bulk modulus $K^e$ (MPa) $K^e = K_f^e(\sigma_3/P^{ref})$	19.80
$\Psi$ (dilation angle) (degrees)	6	Reference effective pressure $p^{ref}$ (kPa)	100
C (cohesion) (kPa)	0	Failure ratio $R_f$	0.97
$K_0$ (lateral earth pressure factor)	0.5	Ultimate friction angle $\varphi_f$ (degrees)	36
Density (kg/m <sup>3</sup> )	1580	Calibration factor $\beta$	1.25

### 3. NUMERICAL MODEL PRESENTATION

The studied wall has a height of 6 meters and is initially composed of four stacked panels, both horizontally and vertically. It is reinforced with eight layers of geosynthetic reinforcements, each 4 meters long [Fig. 2](#).

The front face of the wall has a complex geometry due to the cruciform shape of the panels [Fig.3a](#). To simplify this three-dimensional configuration, a two-dimensional approach is adopted using specific simplifying assumptions. In this model, two panels are considered as the computational width, with four reinforcement strips per panel.

Each panel is represented as a 1.5 m  $\times$  1.5 m square plate, with a uniform distribution of reinforcements [Fig. 3b](#).

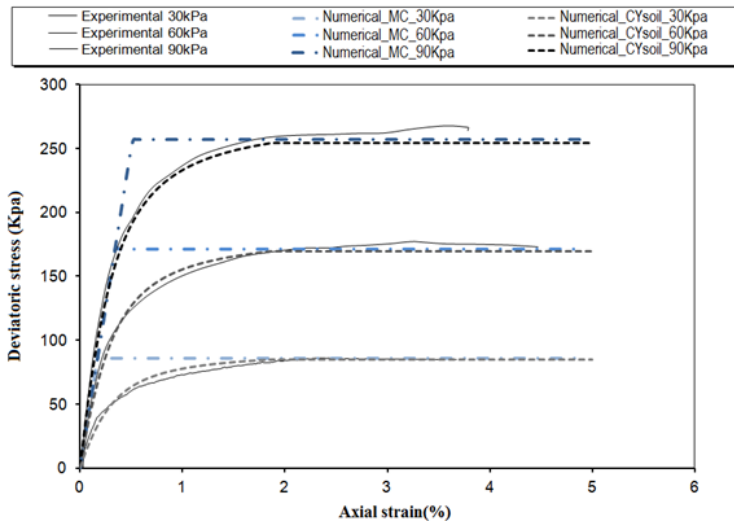


Fig. 1. Calibration of numerical results with experimental tests: Stress-strain relationship.

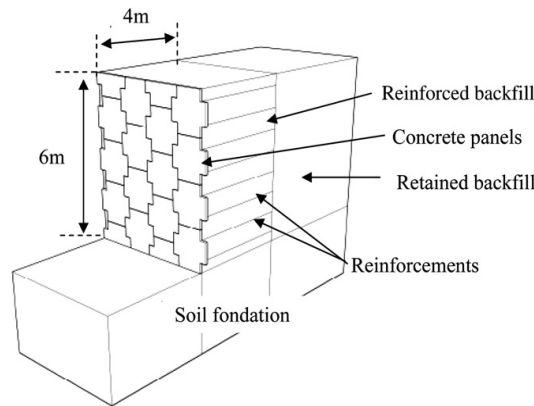


Fig. 2. Schematic Representation of the Studied Reinforced Earth Wall Geometry and Dimensions (Abdelouhab et al., 2011)

The geometric simplification enables the use of a two-dimensional model, where the fibers are assumed to be infinite. The mechanical properties of the fibers can then be scaled according to the characteristics' ratio relative to the width of the examined area Fig. 3c.

For example, the equivalent perimeter of the reinforcements is calculated using the following equation:

$$\text{Reinforcement perimeter} = \frac{2 \times \text{reinforcement width} \times \text{number of reinforcements}}{\text{calculation width}}$$

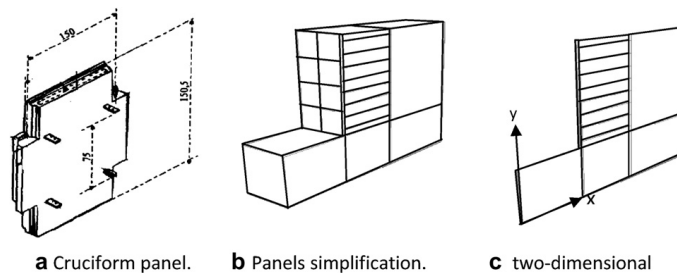


Fig. 3. Two-Dimensional Numerical Model Representation of a Three-Dimensional Reinforced Earth Wall (Abdelouhab et al., 2011)

#### 4. BOUNDARY CONDITIONS AND CONSTRUCTION PHASING

The boundary conditions of the model are defined as follows:

- At the base of the model: Both horizontal and vertical displacements are fully constrained.
- On the lateral sides: Only horizontal displacements are restricted, while vertical movements remain free.

In order to simulate the actual construction accurately, the placing of reinforced and general backfill is modeled in successive 0.375 m layers divided into multiple phases:

- Phase 1: Installation of the first panel, laying of the first and second backfill layers, followed by the installation of the first reinforcement layer between these two layers-equilibrium achieved.
- Phase 2: Laying of the third and fourth backfill layers, followed by placement of the second reinforcement layer (equilibrium achieved).

##### 4.1. Concrete Panels

The concrete panels are modeled in the FLAC 2D code using the beam elements. These panels are considered the facings in the wall for the purpose of retaining stability. In the FLAC 2D code, the mechanical properties, i.e., the elastic modulus, Poisson's ratio, and density of concrete panels, are all set according to experiments conducted on them (Abdelouhab et al., 2011).

It is assumed that the panels behave according to the nonlinear elastic relationship, implying that the panels perform normally in terms of integrity. The properties for the concrete panels are shown in Table 3. It also has to be noted that the interaction between the concrete panels and the soil will be critical for determining the pattern for the deformations that are present.

**Table 3. Mechanical Properties of Concrete Panels (Abdelouhab et al., 2011).**

Parameters	
Constitutive model	Elastic linear
Young modulus (MPa)	15000
Poisson's ratio	0.2
Density (kg/m <sup>3</sup> )	2500

##### 4.2. Soil/Concrete Panel Interface

Interface elements have been incorporated into the model on one side of the panels to represent the stiffness and friction at the interface between the concrete facing and the soil Table 4.

The shear behavior of this interface is described by Coulomb's criterion, which limits the shear force on an element of length  $L$ , according to the following relationship ( Abdelouhab et al., 2012a):

$$F_{smax} = CL + \tan\phi F_n \quad (3)$$

Where:

$F_n$  : Normal force

$c$  : Interface cohesion

$\varphi$  : Interface friction angle

**Table 4. Mechanical Properties of the Concrete Panel/Soil Interface (Abdelouhab et al., 2012a).**

<b>Parameter</b>	
Constitutive model	Coulomb sliding
Normal Stiffness (MPa) at the Facing/Soil Interface	1000
Shear Stiffness (MPa) at the Facing/Soil Interface	1000
Friction Angle at the Facing/Soil Interface (°)	24

The normal and shear stiffness are determined based on FLAC recommendations, while the friction angle is estimated as two-thirds (2/3) of the soil's friction angle.

#### 4.3. Reinforcement

The reinforcement used in the reference model corresponds to GeoStrap 50 (GS 50) geosynthetic strips, which are commonly employed for reinforced soil walls. The mechanical properties incorporated into the model are detailed in Table 5.

In the numerical modeling, the reinforcements are represented using "Strip" structural elements in FLAC2D. These elements are specifically designed to simulate the behavior of reinforcement strips in mechanically stabilized earth walls. The Strip element accounts for:

- Tensile and compressive strength,
- Shear resistance,
- However, it does not support bending moments.

In most practical applications, GeoStrap 50 reinforcements are installed in pairs, with each strip having a width of 50 mm (2 × 50 mm).

**Table 5. Mechanical and Geometrical Characteristics of Reinforcements (GS 50).**

GS 50	
Reinforcements	
Constitutive model	Elastic linear
Elastic modulus (GPa)	2.5
Width (m)	0.1
Thickness (mm)	3
Strip tensile yield-force limit	100
Strip compressive yield force limit	00
Tensile failure strain limit of strip (%)	12

#### 4.4. Soil-Reinforcement Interface

The shear behavior of the soil-reinforcement interface is modeled using a nonlinear law that depends on the confining pressure. Two key parameters characterize this interface:

- The maximum apparent friction coefficient  $f^*$ ,
- The shear stiffness  $k$ .

The maximum apparent friction coefficient at the soil-reinforcement interface is defined as:

$$f^* = \frac{\tau_{max}}{\sigma_{v0}} \quad (4)$$

Where:

- $\sigma_{v0}$  represents the initial normal stress applied to the reinforcement,
- $\tau_{max}$  corresponds to the maximum shear stress along the reinforcement (Schlosser and Guilloux, 1981).

In the numerical model, two coefficients,  $f_0^*$  and  $f_1^*$ , are used to characterize the evolution of  $f^*$  as a function of confining pressure. This method is similar to that used for the internal design of the Mechanically Stabilized Earth wall, following the NF P 94 270 standard.

$$f^* = f_0^* x^{\frac{(120-\sigma_v)}{120}} + f_1^* \frac{\sigma_v}{120} \quad (5)$$

In order to model the behavior of the soil reinforcement interface, a nonlinear law depending on the confining stress  $\sigma_v$ , is established. Two friction coefficients are introduced in the numerical model:

- $f_0^*$ : Apparent friction coefficient at the top of the wall ( $\sigma_v = 0$ ),
- $f_1^*$ : Apparent friction coefficient at a depth of 6 m ( $\sigma_v = 120 \text{ kPa}$ ).

The level of shear stiffness at the soil reinforcement boundary, represented as  $k$ , incorporates these parameters:

- $F_{max}$ : Maximum shear force (tensile force) on the reinforcement,
- $L$ : Length of the reinforcement,
- $U^*$ : Relative displacement between the reinforcement and the soil corresponding to the full mobilization of the reinforcement during a pullout test.

$$k = \frac{F_{max}/L}{U^*} \quad (6)$$

The values adopted for the apparent friction coefficient  $f^*$  and shear stiffness ( $k$ ) in the numerical model were determined by calibration based on laboratory pullout tests. Numerical simulation of pullout tests was performed to identify essential interface parameters for modeling an (MSE) wall.

The interface parameters of the reference numerical model are given in Table 6.

**Table 6. Mechanical Properties of the Soil-Reinforcement Interface.**

Parameter	GS 50
Constitutive model	Coulomb sliding
Apparent friction coefficient at the top of the wall « $f_0^*$ »	1.2
Minimum interface friction coefficient at a depth of 6 m « $f_1^*$ »	0.6
Shear stiffness at the soil strip interface $k_b$ (MN/m <sup>2</sup> /m)	0.22

## 5. RESULTS AND DISCUSSION:

### 5.1. Influence of the Constitutive Model

In the case where data are not available, the comparative analysis carried out in this chapter relies on the results obtained with the CYsoil model, which are taken as a reference.

On the basis of numerical simulations, the differences in wall behavior with diverse constitutive laws are evident [Fig. 5a](#), [5b](#), and [8](#). At the points where the maximum facing displacements occur:

- Between the second and third reinforcement levels with the MC model.
- Between the third and fifth reinforcement levels with the CYsoil model.

A wider deformation zone has been predicted by the more complex CYsoil model, which indicates that the consideration of the non-linearity of the soil is a very important factor in a more accurate modeling of the structural response. These results are in agreement with the studies presented by Hatami and Bathurst ([Hatami and Bathurst, 2006](#)), where the non-linearity of the soil leads to a very accurate prediction of the deformation.

Differences can also be noted regarding the analysis of the shear displacements on the reinforcement/soil interface, as depicted in [Fig. 6a](#) and [6b](#). Namely:

On the other hand, the MC model underestimated the peak shear displacement at the interface between the soil reinforcement. There was 13% less prediction in the MC model than the prediction in the CYsoil model used at the fourth reinforcement level. This happens because the MC model could not adequately explain the variation in stiffness that depends on stress levels, as asserted by Rowe and Skinner ([Skinner and Rowe, 2005](#)).

In contrast, the nonlinear models estimate higher shear displacement, and this agrees with the Bergado and Teerawattanasuk study ([Bergado and Teerawattanasuk, 2008](#)); Bergado and Teerawattanasuk found that strain hardening models are in reality closer to the relationship. Nevertheless, there is a consideration of soil dilatancy prior to failure in the proposed CYsoil model. This aspect implies a reduction of shear displacement. The findings of the above paragraph can be correlated with those of Mašín, who in his studies ([Mašín, 2019](#)) pointed out that “an important aspect of the definition of the behaviour of soils after the yield limit is represented by dilatancy.”

This phenomenon affects the mid-height section of the retaining wall, where the effects of the reinforcement's dilatancy are increased because the displacements are considerable, while the level of confinement is low. A similar phenomenon was noted in the study carried out by ([Ling et al. ,2010](#)), where the study indicated that the effect of the deformation caused by the phenomenon affects the overall stability behavior, mainly in the low-confinement zones.

**Table 7: Difference in Structural Movement Induced by the Influence of the Constitutive Model**

Parameters	CYsoil (A)	MC (B)	A/B (%)
Maximum horizontal displacement of the facing (cm)	10.940	8.372	130.67
Maximum vertical displacement of the facing (cm)	7.576	6.987	108.42
Maximum settlement of the retained soil (cm)	2.544	1.663	152.97
Maximum horizontal stress at the facing (kPa)	35,78	29.16	122.70
Maximum vertical stress at the facing (kPa)	140.00	121.70	115.03

## 5.2. Influence of the Constitutive Model on Settlements and Structural Forces

Fig. 9 shows how important a role is played by this constitutive model in determining accurately enough the settlement on top of the soil in retention. Such a difference of 53% can be identified between the results of maximum values using CYsoil model and results evidenced using MC model in Fig. 9.

These findings can also be observed in other referenced scientific literature (Hatami and Bathurst, 2006), in which researchers detected high values of settlements predicted by nonlinear soil models due to consideration of stiffness variations.

To further demonstrate the effect of the constitutive model on designing mechanically stabilized earth (MSE) structures, plastic zones generated near the facing of the soil are depicted in Fig.7 as per two different constitutive models discussed in this study. CYsoil has generated a plastic zone approximately double in size compared to what is predicted using a plastic model MC. These findings have also been supported by Rowe and Skinner (Skinner and Rowe, 2005), which claims that unlike soil structures predicted using nonlinear models of hardening functions, larger plastic zones of soil tend to occur.

Similarly, Fig. 10 reveals a significant difference in structural forces, particularly:

- The horizontal stress applied to the facing.
- The normal displacement of the facing.

These values are evaluated at the final design stage of the wall. As expected, due to the larger plastic zone development near the facing in the CYsoil model, the horizontal stresses induced in the facing are 23% higher than those obtained with the MC model Fig.10. Similar stress amplification effects were reported by Ling et al. (Ling et al., 2010), who found that strain-hardening models generate larger active pressure zones, increasing horizontal stresses on the facing elements of MSE walls.

This phenomenon can be explained by: Higher external loads acting on the facing in the CYsoil model, caused by the self-weight of the active soil mass within the surrounding plastic zone. This result aligns with findings by Bergado and Teerawattanasuk (Bergado and Teerawattanasuk, 2008), who showed that plasticity-based models result in higher soil pressures due to increased mobilization of the active soil mass.

Greater horizontal stress observed on the facing due to increased external loads from the retained soil, amplified by partial constraint of transverse deformation (Poisson effect). This effect was also observed by Mašin (Mašin, 2019), who highlighted that accounting for pre-failure dilatancy leads to larger horizontal stress concentrations in numerical simulations.

Reduced longitudinal forces associated with the CYsoil model due to the larger vertical displacement of the facing, as illustrated in Fig.7. Similar trends have been observed by other researchers; e.g., Fang and Ishibashi (Fang and Ishibashi, 1986), found that larger deformations in the retaining wall lead to lower values of tension forces in the reinforcement.

## 6. CONCLUSION ON THE INFLUENCE OF THE CONSTITUTIVE MODEL

The results presented above have demonstrated that the Mohr-Coulomb model cannot adequately represent the real behavior of the soil in a design of the mechanically stabilized earth walls. The results of the research have the following major findings:

- The MC model underestimates the structural forces, which could cause an unsafe estimate of the stability of the walls.
- The greatest gaps between MC and CYsoil model predictions are in displacement and stress calculations, with the least gap in vertical stress calculations Table 7.
- CYsoil indicates the extent of the plastic deformation zone; from this perspective too, the nonlinear character of the soil's behavior can be considered essential for an exact assessment.
- The findings again support previous studies carried out on similar topics by other researchers and authors confirm previous findings (Bolton and Lau, 1993; Addenbrooke et al., 1997; Ling et al., 2009; Lambrughi et al., 2012; Do et al., 2013a; Seyedi Hosseininia, 2015; Rodriguez et al., 2018; Salih et al., 2022), which highlight the limitations of the MC model in capturing stress-dependent stiffness variations.
- The adoption of a nonlinear model such as CYsoil allows for a more realistic representation of soil behavior, leading to safer and more reliable designs for MSE walls.

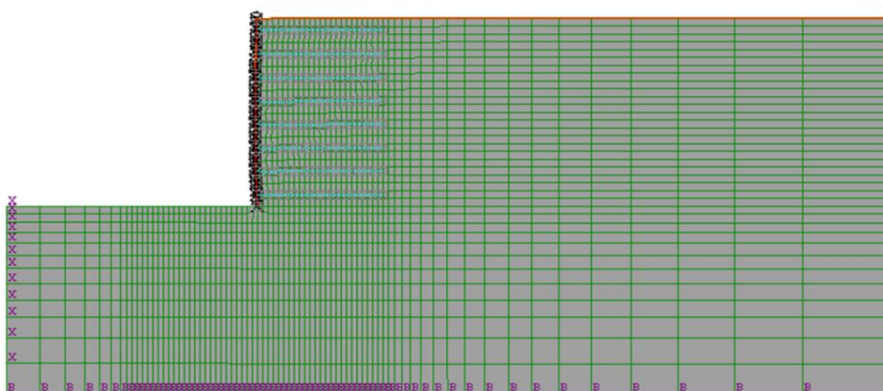


Fig. 4. View of the numerical model developed in FLAC2D.

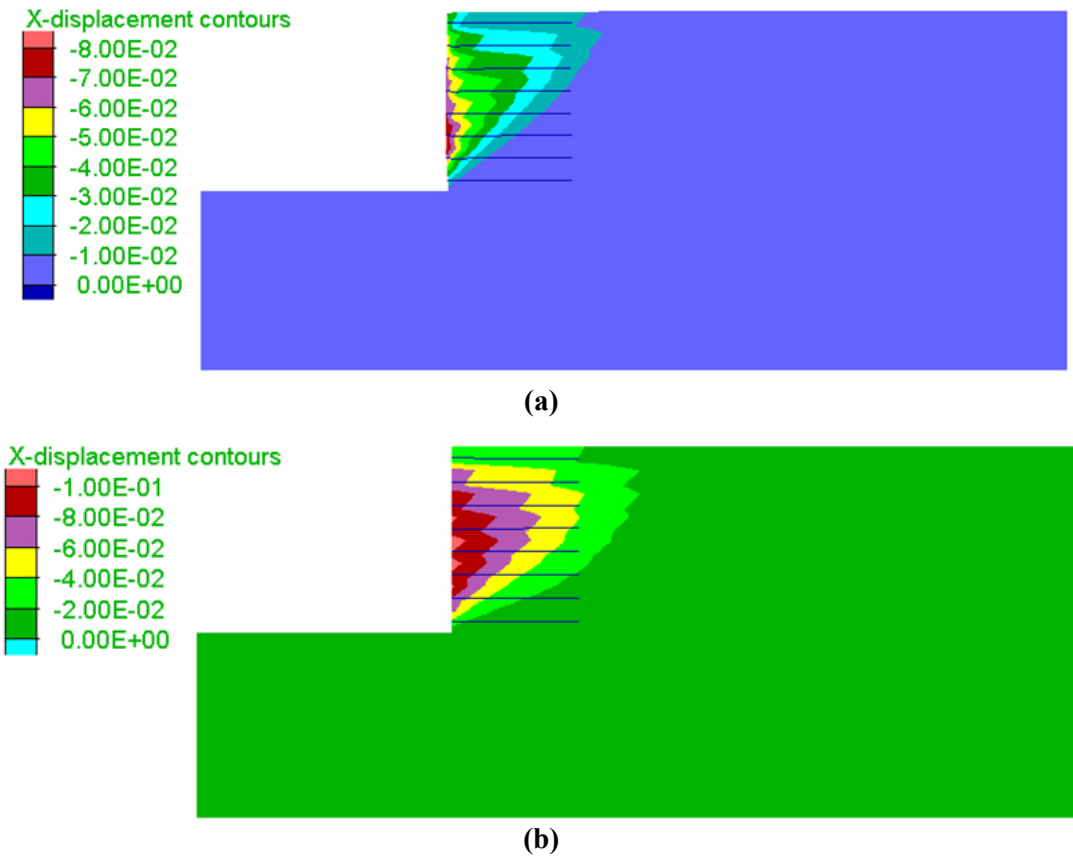


Fig. 5. Horizontal displacements of the facing: a) MC model; b) CYsoil model.

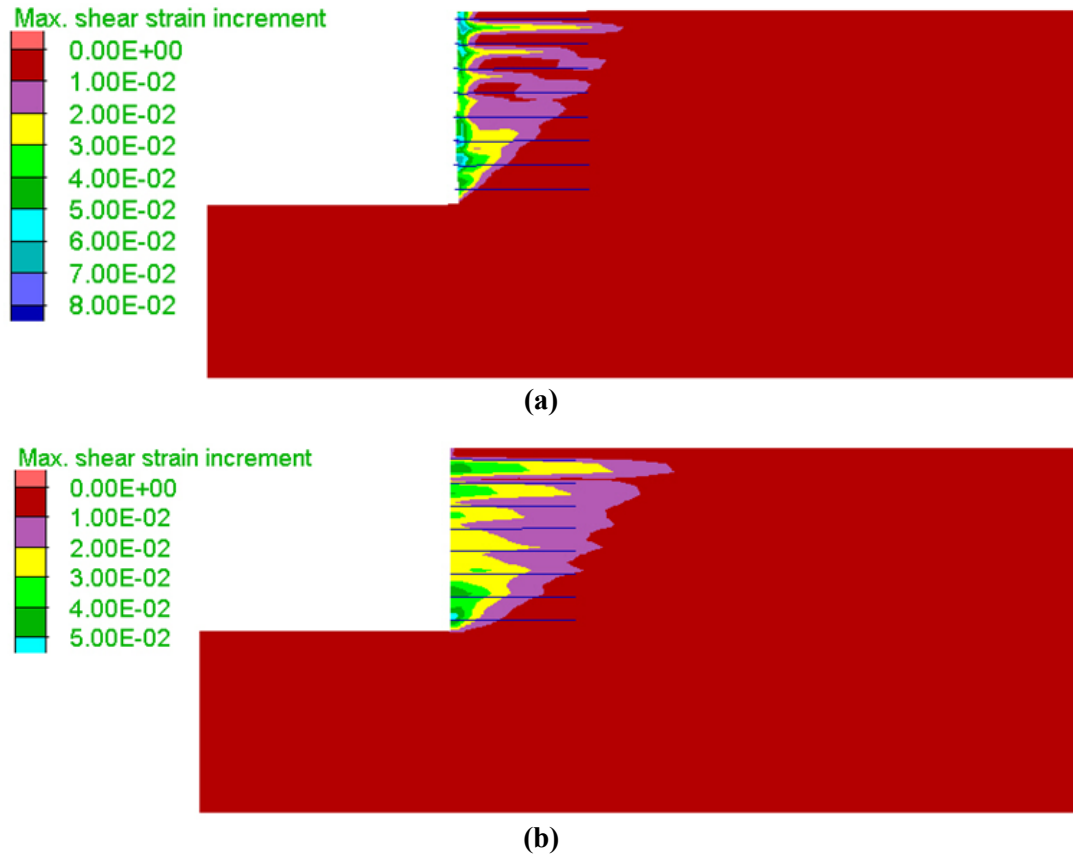
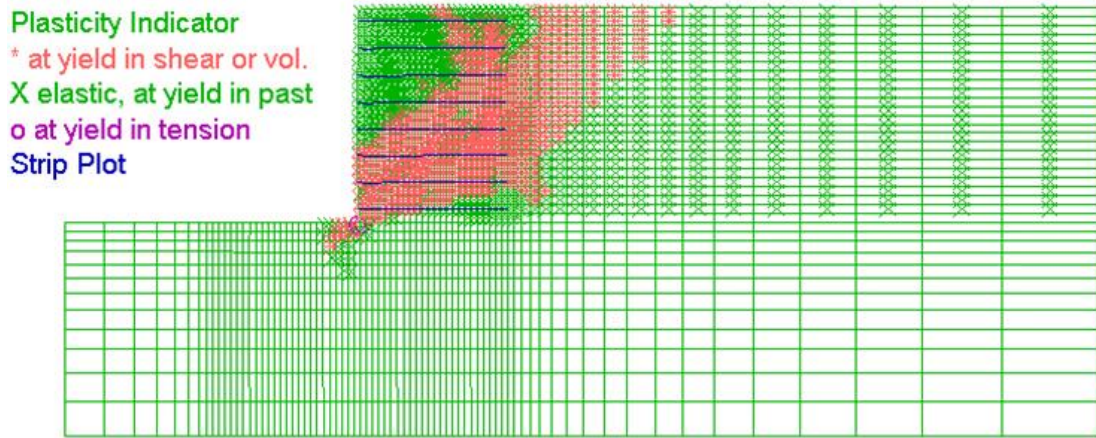
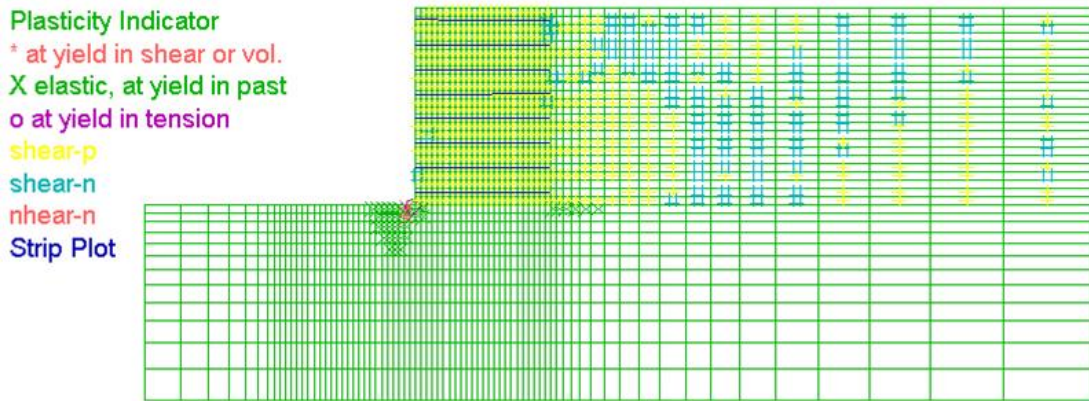


Fig. 6. Shear stress : (a) MC model; (b) CYsoil model.



(a)



(b)

Fig. 7. Plastic zone : (a) MC model; (b) CYsoil model.

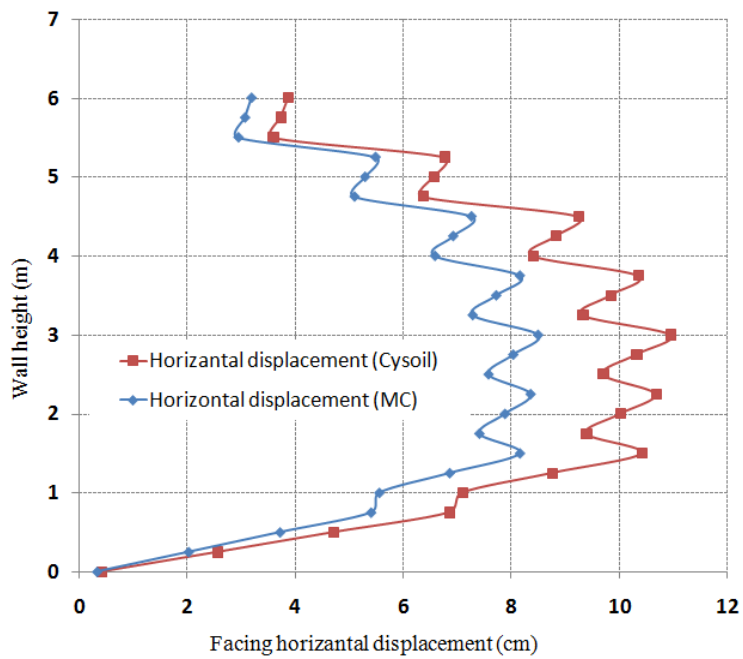


Fig. 8. Comparison of horizontal displacements.

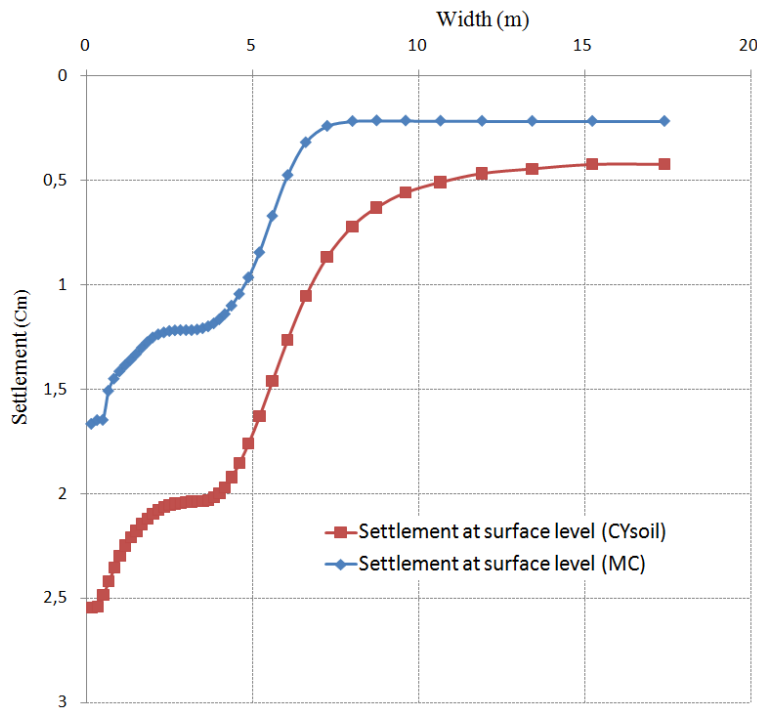


Fig. 9. Comparison of the settlement of the retained soil.

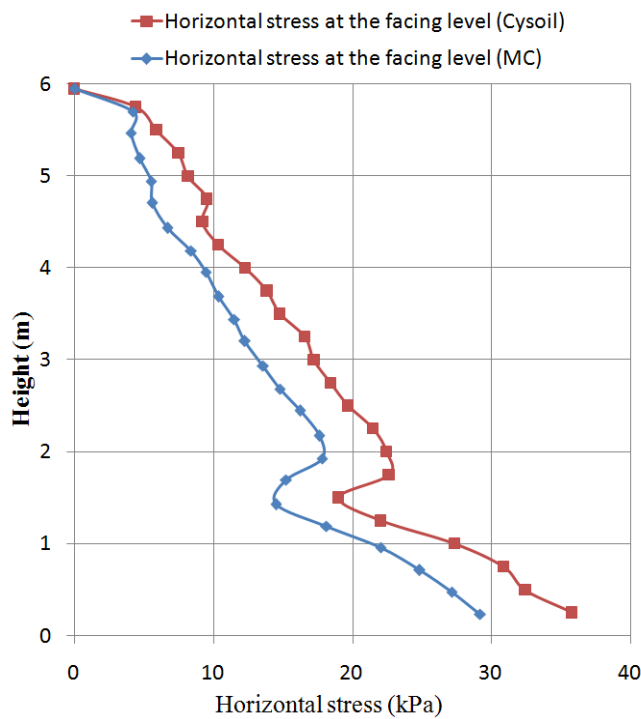


Fig. 10. Comparison of horizontal stresses at the facing

### 7. CONCLUSION

A two-dimensional numerical model was developed to simulate the design process of a reinforced earth wall (REW). This model accurately predicts soil movements as well as the structural forces induced at the facing.

In this study, two soil constitutive models were compared in the numerical modeling of the wall:

- Mohr-Coulomb (MC) model: A linear elasto-plastic model.
- CYsoil model: A nonlinear elastic model that accounts for stress-strain nonlinearity and soil dilatancy.

The comparative analysis of numerical results and experimental measurements led to the following observations:

- Both models are capable of reproducing the overall deformation pattern of the REW wall. However, the model that more accurately describes soil behavior in terms of stress and strain provides a better match with experimental triaxial calibration data.
- Accurate prediction of facing displacements requires a rigorous consideration of both elastic and plastic deformation parameters of the soil constitutive model.
- In a nonlinear model, an appropriate distribution of soil elastic stiffness improves the accuracy of wall deformation predictions.
- Dilative parameters significantly influence wall deformation. A contractive soil behavior rather than a dilative one provides more realistic predictions of facing displacements. A reasonable correlation between shear strength and dilatancy parameters is essential.
- Selection of the constitutive model influences the determination of the lateral stresses behind the wall, as well as the applied stresses on the foundation.

The results highlight the effect of the soil behavior model on the displacements of the structural elements or the surrounding soils. Generally, the structural elements are subjected to more forces with displacement according to the CYsoil model compared with the MC model. Thus, the necessity of the advanced model in the geotechnical study is emphasized, highlighting the capability of the model in the reliable analysis of the reinforced earth structure.

## 8. REFERENCES

Abdelouhab, A., Dias, D. and Freitag, N., (2011). Numerical analysis of the behaviour of mechanically stabilized earth walls reinforced with different types of strips. *Geotextiles and Geomembranes*, 29(2), pp.116-129. doi:<https://doi.org/10.1016/j.geotexmem.2010.10.011>.

Abdelouhab, A., Dias, D. and Freitag, N., (2012a). Modélisation physique et analytique de renforcements extensibles–Développement d’une nouvelle armature. *European journal of environmental and civil engineering*, 16(10), pp.1115-1142. doi:<https://doi.org/10.1080/19648189.2012.666904>.

Abdelouhab, A., Dias, D. and Freitag, N., (2012b). Modélisation numérique bidimensionnelle de murs en Terre Armée. *European journal of environmental and civil engineering*, 16(10), pp.1143-1167. doi:<https://doi.org/10.1080/19648189.2012.666908>.

Abdulhasan, O., Mustafa, F. and Al-Zuhairi, A., (2020). Performance of skirted circular shallow footings resting on sandy soil under inclined loads. *Kufa Journal of Engineering*, 11(2), pp.10-27. doi:<https://doi.org/10.30572/2018/KJE/110202>.

Addenbrooke, T.I., Potts, D.M. and Puzrin, A.M. (1997). The influence of pre-failure soil stiffness on the numerical analysis of tunnel construction. *Géotechnique*, 47(3), pp.693–712. doi:<https://doi.org/10.1680/geot.1997.47.3.693>.

Allen, T.M. and Bathurst, R.J., (2015). Improved simplified method for prediction of loads in reinforced soil walls. *Journal of Geotechnical and Geoenvironmental Engineering*, 141(11), p.04015049. doi:[https://doi.org/10.1061/\(ASCE\)GT.1943-5606.0001355](https://doi.org/10.1061/(ASCE)GT.1943-5606.0001355).

Angel, M., Magna-Verdugo, C. and Abell, J.A. (2018). Influence of Soil-Structure-Interaction in Shear-wall RC Buildings Fragility Curves. [online] ResearchGate. Available at: [https://www.researchgate.net/publication/326881587\\_Influence\\_of\\_Soil-Structure-Interaction\\_in\\_Shear-wall\\_RC\\_Buildings\\_Fragility\\_Curves](https://www.researchgate.net/publication/326881587_Influence_of_Soil-Structure-Interaction_in_Shear-wall_RC_Buildings_Fragility_Curves).

BASTICK, M. (2025). L'apport de la méthode des éléments finis à l'étude du comportement des ouvrages en terre armée. [online] pp.257–263. Available at: <http://pascal-francis.inist.fr/vibad/index.php?action=getRecordDetail&idt=7338836>.

Bathurst, R.J. and Naftchali, F.M., (2021). Geosynthetic reinforcement stiffness for analytical and numerical modelling of reinforced soil structures. *Geotextiles and Geomembranes*, 49(4), pp.921-940. doi:<https://doi.org/10.1016/j.geotexmem.2021.01.003>.

Bergado, D.T. and Teerawattanasuk, C., (2008). 2D and 3D numerical simulations of reinforced embankments on soft ground. *Geotextiles and Geomembranes*, 26(1), pp.39-55. doi:<https://doi.org/10.1016/j.geotexmem.2007.03.003>.

Bolton, M.D. and Lau, C.K., (1993). Vertical bearing capacity factors for circular and strip footings on Mohr–Coulomb soil. *Canadian Geotechnical Journal*, 30(6), pp.1024-1033. doi:<https://doi.org/10.1139/t93-09>.

Brahim Lafifi, Hamrouni, A., Tarek Khoualdia, Abderrahim Gheris and Ammar Rouaiguia (2024). Prediction and optimization of the bearing capacity of strip footing resting on soft soil

improved with stone columns using RSM, ANN, and multi-objective GA. *Innovative Infrastructure Solutions*, 9(5). doi:<https://doi.org/10.1007/s41062-024-01452-2>.

Chang, J.C. and Forsyth, R.A., (1977). Finite element analysis of reinforced earth wall. *Journal of the Geotechnical Engineering Division*, 103(7), pp.711-724. doi:<https://doi.org/10.1061/AJGEB6.00004>.

Clough, G.W. and Duncan, J.M., (1971). Finite element analyses of retaining wall behavior. *Journal of the Soil Mechanics and Foundations Division*, 97(12), pp.1657-1673. doi:<https://doi.org/10.1061/JSFEAQ.00017>

Do, N.-A., Dias, D., Oreste, P. and Djeran-Maigre, I. (2013). Three-dimensional numerical simulation for mechanized tunnelling in soft ground: the influence of the joint pattern. *Acta Geotechnica*, 9(4), pp.673–694. doi:<https://doi.org/10.1007/s11440-013-0279-7>.

Fang, Y. and Ishibashi, I. (1986). Static Earth Pressures with Various Wall Movements. *Journal of Geotechnical Engineering*, 112(3), pp.317–333. doi:[https://doi.org/10.1061/\(asce\)0733-9410\(1986\)112:3\(317\)](https://doi.org/10.1061/(asce)0733-9410(1986)112:3(317)).

Fathipour, H., Safardoost Siahmazgi, A., Payan, M., Jamshidi Chenari, R. and Veiskarami, M. (2023). Evaluation of the Active and Passive Pseudo-dynamic Earth Pressures using Finite Element Limit Analysis and Second-order Cone Programming. *Geotechnical and Geological Engineering*, 41(3), pp.1921–1936. doi:<https://doi.org/10.1007/s10706-023-02381-0>.

Flavigny, E., Desrues, J. and Palayer, B. (1990). Note technique : le sable d'Hostun 'RF'. *Revue Française de Géotechnique*, [online] (53), pp.67–70. doi:<https://doi.org/10.1051/geotech/1990053067>.

Gay, O., Boutonnier, L., Guerpillon, Y., Foray, P. and Flavigny, E. (2001). Modélisation physique et numérique de l'action d'un glissement lent sur des fondations d'ouvrages d'art. *Revue Française de Géotechnique*, (95-96), pp.75–86. doi:<https://doi.org/10.1051/geotech/2001095075>.

Hamrouni, A., Dias, D. and Guo, X. (2022). Behavior of Shallow Circular Tunnels—Impact of the Soil Spatial Variability. *Geosciences*, 12(2), p.97. doi:<https://doi.org/10.3390/geosciences12020097>.

Hatami, K. and Bathurst, R.J. (2006). Numerical Model for Reinforced Soil Segmental Walls under Surcharge Loading. *Journal of Geotechnical and Geoenvironmental Engineering*, 132(6), pp.673–684. doi:[https://doi.org/10.1061/\(asce\)1090-0241\(2006\)132:6\(673\)](https://doi.org/10.1061/(asce)1090-0241(2006)132:6(673)).

- Helwany, S.M.B., Reardon, G. and Wu, J.T.H. (1999). Effects of backfill on the performance of GRS retaining walls. *Geotextiles and Geomembranes*, 17(1), pp.1–16. doi:[https://doi.org/10.1016/s0266-1144\(98\)00021-1](https://doi.org/10.1016/s0266-1144(98)00021-1).
- Ho, S.K. and Rowe, R.K. (1994). Predicted Behavior of Two Centrifugal Model Soil Walls. *Journal of Geotechnical Engineering*, 120(10), pp.1845–1873. doi:[https://doi.org/10.1061/\(asce\)0733-9410\(1994\)120:10\(1845\)](https://doi.org/10.1061/(asce)0733-9410(1994)120:10(1845)).
- Hu, J. and Li, X. (2024). A novel prediction model construction and result interpretation method for slope deformation of deep excavated expansive soil canals. *Expert Systems with Applications*, 236, p.121326. doi:<https://doi.org/10.1016/j.eswa.2023.121326>.
- Itasca, I., 2011. *FLAC (Fast Lagrangian Analysis of Continua) Version 7.0*. Minneapolis, Minnesota: Itasca Consulting Group.
- L. Hayal, A., M.B. Al-Gharrawi, A. and Y. Fattah, M. (2021). Effect of nanomaterials on shear strength of gypseous soil. *Kufa Journal of Engineering*, 12(1). doi:<https://doi.org/10.30572/2018/kje/120101>.
- Lambrughi, A., Medina Rodríguez, L. and Castellanza, R. (2012). Development and validation of a 3D numerical model for TBM–EPB mechanised excavations. *Computers and Geotechnics*, 40, pp.97–113. doi:<https://doi.org/10.1016/j.compgeo.2011.10.004>.
- Ling, H.I. and Liu, H. (2009). Deformation analysis of reinforced soil retaining walls—simplistic versus sophisticated finite element analyses. *Acta Geotechnica*, 4(3), pp.203–213. doi:<https://doi.org/10.1007/s11440-009-0091-6>.
- Ling, H.I., Yang, S., Dov Leshchinsky, Liu, H. and Burke, C. (2010). Finite-Element Simulations of Full-Scale Modular-Block Reinforced Soil Retaining Walls under Earthquake Loading. *Journal of Engineering Mechanics-asce*, 136(5), pp.653–661. doi:[https://doi.org/10.1061/\(asce\)em.1943-7889.0000108](https://doi.org/10.1061/(asce)em.1943-7889.0000108).
- Liu, H. (2016). Nonlinear Elastic Analysis of Reinforcement Loads for Vertical Reinforced Soil Composites without Facing Restriction. *Journal of Geotechnical and Geoenvironmental Engineering*, 142(6), p.04016013. doi:[https://doi.org/10.1061/\(asce\)gt.1943-5606.0001464](https://doi.org/10.1061/(asce)gt.1943-5606.0001464).
- Liu, H., Wang, X. and Song, E. (2011). Reinforcement load and deformation mode of geosynthetic-reinforced soil walls subject to seismic loading during service life. *Geotextiles and Geomembranes*, 29(1), pp.1–16. doi:<https://doi.org/10.1016/j.geotexmem.2010.06.003>.

- Maji, V.B., Sowmiyaa, V.S. and Robinson, R.G. (2016). A Simple Analysis of Reinforced Soil Using Equivalent Approach. *International Journal of Geosynthetics and Ground Engineering*, 2(2). doi:<https://doi.org/10.1007/s40891-016-0055-5>.
- Mašín, D. (2019). *Modelling of Soil Behaviour with Hypoplasticity*. Springer Series in Geomechanics and Geoengineering. Cham: Springer International Publishing. doi:<https://doi.org/10.1007/978-3-030-03976-9>.
- Morsy, A.M. and Zornberg, J.G. (2021). Soil-reinforcement interaction: Stress regime evolution in geosynthetic-reinforced soils. *Geotextiles and Geomembranes*, 49(1), pp.323–342. doi:<https://doi.org/10.1016/j.geotexmem.2020.08.007>.
- Pande, G.N. and S. Pietruszczak (2021). A critical look at constitutive models for soils. *Routledge eBooks*, pp.369–393. doi:<https://doi.org/10.1201/9780203753583-19>.
- Pham, T.A. and Dias, D. (2021). 3D numerical study of the performance of geosynthetic-reinforced and pile-supported embankments. *Soils and Foundations*. doi:<https://doi.org/10.1016/j.sandf.2021.07.002>.
- S. Yousif, A. and S. Mustafa, F. (2021). BEHAVIOR OF SALINE SOIL STABILIZED WITH POLYPROPYLENE FIBER AND CEMENT. *Kufa Journal of Engineering*, 12(1). doi:<https://doi.org/10.30572/2018/kje/120103>.
- Salih, A.G., Ahmad and Salih, N.B. (2022). Finite Element Analysis of the Load-Settlement Behavior of Large-Scale Shallow Foundations on Fine-Grained Soil Utilizing Plaxis 3D. pp.249–260. doi:[https://doi.org/10.1007/978-981-19-7358-1\\_22](https://doi.org/10.1007/978-981-19-7358-1_22).
- Schlösser, F. and Guilloux, A. (1981). Le frottement dans le renforcement des sols. *Revue Française de Géotechnique*, (16), pp.65–77. doi:<https://doi.org/10.1051/geotech/1981016065>.
- Seyedi Hosseininia, E. (2015). A micromechanical study on the stress rotation in granular materials due to fabric evolution. *Powder Technology*, 283, pp.462–474. doi:<https://doi.org/10.1016/j.powtec.2015.06.013>.
- Seyedi Hosseininia, E. and Ashjaee, A. (2018). Numerical simulation of two-tier geosynthetic-reinforced-soil walls using two-phase approach. *Computers and Geotechnics*, 100, pp.15–29. doi:<https://doi.org/10.1016/j.compgeo.2018.04.003>.
- Skinner, G.D. and Kerry Rowe, R. (2005). Design and behaviour of a geosynthetic reinforced retaining wall and bridge abutment on a yielding foundation. *Geotextiles and Geomembranes*, 23(3), pp.234–260. doi:<https://doi.org/10.1016/j.geotexmem.2004.10.001>.

Vibhoosha, M.P., Anjana Bhasi and Nayak, S. (2021). A Review on the Design, Applications and Numerical Modeling of Geocell Reinforced Soil. *Geotechnical and Geological Engineering*, 39(6), pp.4035–4057. doi:<https://doi.org/10.1007/s10706-021-01774-3>.

Xie, M., Li, L., Cao, W., Zheng, J. and Dong, X. (2022). Centrifugal and numerical modeling of embankment widening over soft soils treated by pile-supported geosynthetic-reinforced soil wall. *Acta Geotechnica*, 18(2), pp.829–841. doi:<https://doi.org/10.1007/s11440-022-01611-8>.

Yang, X., Han, J., Parsons, R.L. and Dov Leshchinsky (2010). Three-dimensional numerical modeling of single geocell-reinforced sand. *Frontiers of Architecture and Civil Engineering in China*, 4(2), pp.233–240. doi:<https://doi.org/10.1007/s11709-010-0020-7>.

Yu, Y., Bathurst, R.J. and Miyata, Y. (2015). Numerical analysis of a mechanically stabilized earth wall reinforced with steel strips. *Soils and Foundations*, 55(3), pp.536–547. doi:<https://doi.org/10.1016/j.sandf.2015.04.006>.

Zhang, F., Zhu, Y., Chen, Y. and Yang, S. (2021). Seismic effects on reinforcement load and lateral deformation of geosynthetic-reinforced soil walls. *Frontiers of Structural and Civil Engineering*, 15(4), pp.1001–1015. doi:<https://doi.org/10.1007/s11709-021-0734-8>.

Zhang, J., Jenck, O. and Dias, D. (2022). 3D Numerical Analysis of a Single Footing on Soft Soil Reinforced by Rigid Inclusions. *International Journal of Geomechanics*, 22(8). doi:[https://doi.org/10.1061/\(asce\)gm.1943-5622.0002412](https://doi.org/10.1061/(asce)gm.1943-5622.0002412).

Zienkiewicz, O.C., Humpheson, C. and Lewis, R.W. (1975). Associated and non-associated visco-plasticity and plasticity in soil mechanics. *Géotechnique*, 25(4), pp.671–689. doi:<https://doi.org/10.1680/geot.1975.25.4.671>.